Solution Studies of Isepamicin and Conformational Comparisons between Isepamicin and Butirosin A When Bound to an Aminoglycoside 6′-*N*-Acetyltransferase Determined by NMR Spectroscopy

Enrico L. DiGiammarino,[‡] Kari-ann Draker,[§] Gerard D. Wright,[§] and Engin H. Serpersu*,[‡]

Department of Biochemistry, Cellular and Molecular Biology, University of Tennessee, Knoxville, Tennessee 37996-0840 and Department of Biochemistry, McMaster University, 1200 Main Street West, Hamilton, Ontario, Canada L8N 3Z5

Received November 12, 1997; Revised Manuscript Received January 12, 1998

ABSTRACT: NMR spectroscopy, combined with molecular modeling, was used to determine the conformations of isepamicin and butirosin A in the active site of aminoglycoside 6′-*N*-acetyltranferase-Ii [AAC(6′)-Ii]. The results suggest two enzyme-bound conformers for isepamicin and one for butirosin A. The dihedral angles that describe the glycosidic linkage between the A and B rings for the two conformers of AAC(6′)-Ii-bound isepamicin were $\phi_{AB} = -7.9 \pm 2.0°$ and $\psi_{AB} = -46.2 \pm 0.6°$ for conformer 1 and $\phi_{AB} = -69.4 \pm 2.0°$ and $\psi_{AB} = -57.7 \pm 0.5°$ for conformer 2. Unrestrained molecular dynamics calculations showed that these distinct conformers are capable of interconversion at 300 K. When superimposed at the 2-deoxystreptamine ring, one enzyme-bound conformer of isepamicin (conformer 1) places the reactive 6′ nitrogen in a similar position as that of butirosin A. Conformer 2 of AAC(6′)-Ii-bound isepamicin may represent an unproductive binding mode. Unproductive binding modes (to aminoglycoside modifying enzymes) could provide one reason isepamicin remains one of the more effective aminoglycoside antibiotics. The enzyme-bound conformation of butirosin A yielded an orthogonal arrangement of the 2,6-diamino-2,6-dideoxy-D-glucose and D-xylose rings, as opposed to the parallel arrangement which was observed for this aminoglycoside in the active site of an aminoglycoside 3′-*O*-phosphotransferase [Cox, J. R., and Serpersu, E. H. (1997) *Biochemistry 36*, 2353−2359]. The complete proton and carbon NMR assignments of the aminoglycoside antibiotic isepamicin at pH 6.8 as well as the pK_a values for it's amino groups are also reported.

Aminoglycosides are a class of antibiotics used for treatment against staphylococci, a variety of Gram-negative bacteria and Gram-positive bacilli (*1*). Their primary target is the 16S rRNA of the 30S ribosomal subunit, binding to which results in disruption of normal protein biosynthesis, eventually leading to cell death. However, as with most antibiotics, bacterial resistance to aminoglycosides has become increasingly problematic (*2*). While there are several mechanisms by which resistance can arise, the most clinically relevant resistance mechanism is enzymatic inactivation of aminoglycosides by *N*-acetyltransferases (AAC), *O*-nucleotidyltransferases (ANT), and *O*-phosphotransferases (APH) (*3*, *4*). Over 50 different aminoglycoside modifying enzymes among the three classes have been identified (*3*). Many individual enzymes within each class can modify a broad range of aminoglycosides. Investigations of the modes by which aminoglycosides bind to their modifying enzymes may provide valuable insight into important structural and conformational characteristics that give rise to broad substrate specificity.

Two major families of aminoglycosides are disubstituted at positions 4 and 5 or 4 and 6 at the 2-deoxystreptamine ring. Isepamicin, a semisynthetic derivative of the gentamicin B, and butirosin A were used in this study as representatives of the two major families of aminoglycosides (Figure 1). The A rings (or primed rings) in isepamicin and butirosin A are 6-amino-6-deoxy-D-glucose and 2,6-diamino-2,6-dideoxy-D-glucose, respectively. The B rings (or unprimed rings) are 2-deoxystreptamine modified at position $N - 1$ with an (*S*)-3-amino-2-hydroxypropionyl group in isepamicin and an (*S*)-4-amino-2-hydroxybutyryl group in butirosin A, which are denoted with the letter D (or triple-prime). The C ring (or double-primed ring) in isepamicin is D-garosamine and in butirosin A is D-xylose.

The most common aminoglycoside modifying enzymes in pathogenic Gram-negative bacteria are the 6′-*N*-acetyltransferases (*5*). Recently, a chromosomally encoded aminoglycoside 6′-*N*-acetyltransferase [AAC(6′)-Ii] from *Enterococcus faecium* has been cloned, overexpressed, and characterized (*6*). This enzyme catalyzes the regiospecific acetyl transfer from acetylCoA to the 6_A (or 6′) nitrogen of aminoglycosides with free 6_A amine groups rendering these antibiotics inoffensive. The enzyme confers resistance to

* To whom correspondence should be addressed. Phone: 423-974-2668. Fax: 423-974-6306. E-mail: serpersu@bionmr.bio.utk.edu.

[‡] University of Tennessee.

[§] McMaster University.

[1] Abbreviations: AAC, aminoglycoside acetyltransferase; ANT, aminoglycoside nucleotidyltransferase; APH, aminoglycoside phosphotransferase; COSY, correlated spectroscopy; HOHAH, Ahomonuclear Hartmann−Hahn spectroscopy; NOESY, nuclear Overhauser effect spectroscopy; rmsd, root-mean-square deviation; TRNOESY, transferred nuclear Overhauser effect spectroscopy.

S0006-2960(97)02778-5 CCC: $15.00
Published on Web 02/26/1998

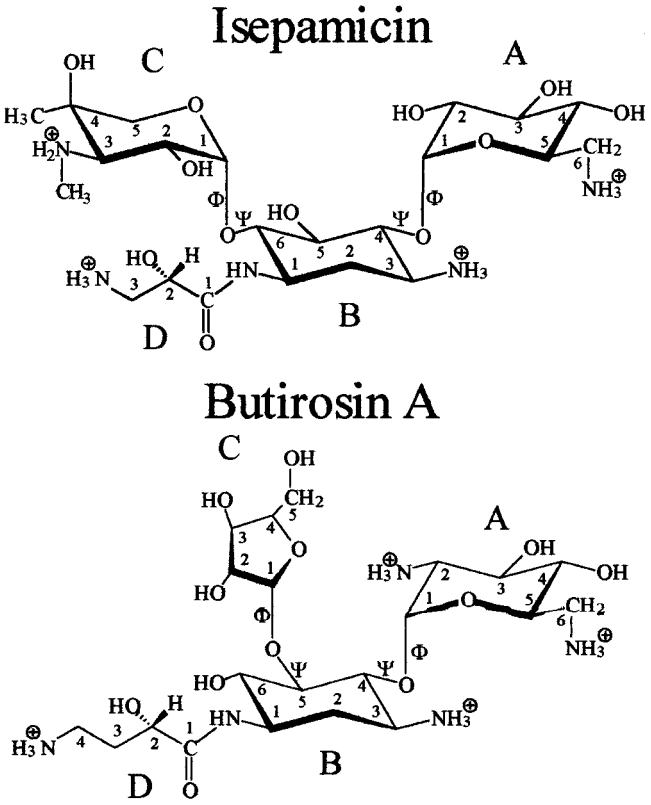

FIGURE 1: The structures of isepamicin and butirosin A. The ring/chain designations A, B, C, and D are also referred to as primed, unprimed, double primed, and triple primed, respectively. The bonds about which rotation describes the glycosidic angles of Phi (ϕ) and Psi (ψ) are indicated.

low levels (minimal inhibitory concentrations) of aminoglycosides in *E. faecium* and is known to modify a wide range of aminoglycoside substrates, among which are butirosin A (*6*) and isepamicin (this work). In this manuscript, we report AAC(6′)-Ii-bound conformations of isepamicin and butirosin A determined by transferred nuclear Overhauser effect spectroscopy (TRNOESY) and molecular modeling.

MATERIALS AND METHODS

Materials. Isepamicin (sulfate salt) was a gift from Drs. K. Shaw and G. Miller of Schering Plough. Butirosin A (sulfate salt) was a gift from Dr. D. C. Baker of The University of Tennessee, Knoxville. Coenzyme A was purchased from Sigma. Sulfate was removed from aminoglycosides by precipitation with equimolar BaOH. AAC(6′)-Ii was purified as described previously (*6*). D_2O was from Cambridge Isotope Laboratories and deuterated Tris (Tris-d_{11}), deuterium chloride, and sodium deuterioxide were from Isotec.

Kinetics. Kinetic parameters of isepamicin acetylation by AAC(6′)-Ii were determined by CoASH titration as previously described (*6*).

NMR Spectroscopy. All NMR spectra were obtained with a wide-bore Bruker AMX 400 MHz spectrophotometer at 27 °C. All proton chemical shifts were referenced to 2,2-dimethyl-2-silapentane-5-sulfonate (DSS), carbon chemical shifts were referenced against TMS, and ^{15}N chemical shifts were referenced against $^{15}NH_4Cl$.

Proton resonance assignments of isepamicin were made using homonuclear COSY, NOESY, and HOHAHA (homonuclear Hartmann−Hahn spectroscopy) (*7*−*9*) experiments. Data sets were collected in the phase sensitive mode using the time-proportional phase increment method (*10*). A total of 207−256 FIDs of 2K data were collected. The spectral width was 4032.26 Hz and 32 scans per FID were acquired. Mixing times of 37, 76, and 123 ms were employed in HOHAHA experiments. A mixing time of 300 ms was used in NOESY experiments with free isepamicin. Mixing times of 60, 90, 120, and 150 ms were used in NOESY experiments with enzyme-bound isepamicin. The data were zero filled to 0.5K or 1K points in t_1 and were multiplied by sine (COSY) or sine^2 (HOHAHA, NOESY) window functions in both dimensions before Fourier transformation. A data matrix of 2K × 256 was acquired for ^{13}C-^1H COSY experiments (*11*−*13*). Proton decoupling was achieved with the WALTZ 16 sequence (*14*), and 32 transients were obtained for each value of t_1. The data were zero filled to 512 points in t_1 and Gaussian multiplication was used in both dimensions.

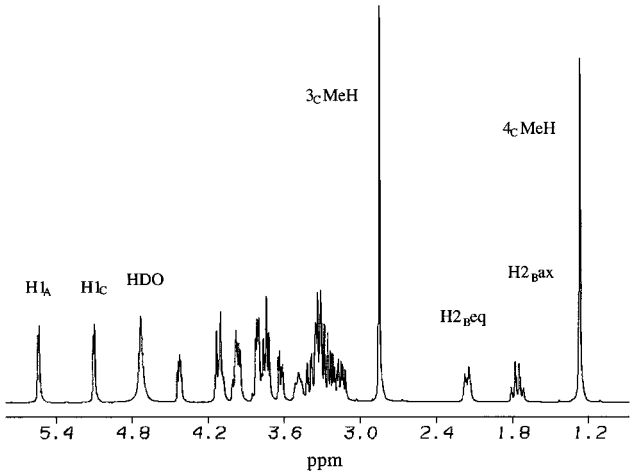

FIGURE 2: 1D ^1H NMR spectrum of isepamicin at pH 6.8. The anomeric proton resonances ($H1_A$ and $H1_C$), $H2_B$ axial and equatorial resonances, and 3_C and 4_C methyl proton resonances are indicated.

The 1-D proton NMR spectrum of isepamicin is shown in Figure 2, and proton and carbon resonance assignments of isepamicin are given in Table 1.

Using previously published assignments (*15*), ^{15}N resonances were monitored as a function of pH to determine the pK_a values of the amine groups (Table 2). The amide proton at $N1_B$ did not titrate over the pH values used in this study (pH 4.8−12.4). The pK_a values were determined by fitting the data to a modified Hill equation (*16*) using the program P-Fit (Biosoft), and all Hill coefficients were less than one. The proton NMR spectral assignments for butirosin A and the solution structure at pH 6.5 have been previously reported (*17*).

AAC(6′)-Ii was dialyzed against 1 mM Tris-d_{11}, pH 6.8, and the enzyme was then cycled through lyophilization followed by redissolving in D_2O three times. Isepamicin, butirosin A, and coenzyme A were also cycled through lyophilization followed by redissolving in D_2O three times. Samples for TRNOESY experiments contained 0.30 mM AAC(6′)-Ii, 3−10 mM isepamicin or butirosin A, 1−6 mM coenzyme A, and 2 mM Tris-d_{11} buffer (pH 6.8). Several experiments were performed. The NMR data was analyzed by FELIX 95 software package (BIOSYM/Molecular Simu-

Table 1: ^{1}H NMR Chemical Shifts (ppm) and ^{13}C NMR Chemical Shifts (ppm) for Isepamicin

proton	chemical shift (ppm)	carbon	chemical shift (ppm)
1A	5.53	1A	92.93
2A	3.63	2A	67.85
3A	3.74	3A	69.13
4A	3.34	4A	67.85
5A	3.98	5A	65.57
6A	3.40	6A	37.40
6A	3.16		
1B	4.10	1B	45.65
2Bax	1.76	2B	27.59
2Beq	2.16	3B	45.07
3B	3.47	4B	76.27
4B	3.80	5B	69.73
5B	3.82	6B	77.05
6B	3.74		
1C	5.10	1C	95.19
2C	3.95	2C	63.04
3C	3.27	3C	61.33
3CMe	2.85	3CMe	32.28
4CMe	1.28	4C	66.95
5Ceq	4.14	4CMe	18.10
5Cax	3.35	5C	63.80
2D	4.43	1D	169.65
3D	3.31	2D	64.72
3D	3.23	3D	38.85

Table 2: pK_a Values[a] of the Amino Groups of Isepamicin

amine group nitrogen	pK_a	most downfield δ (ppm)	most upfield δ (ppm)
N6A	8.68 ± 0.01[b]	16.05 ± 0.17[c]	9.29 ± 0.21
N3B	7.63 ± 0.07	10.52 ± 0.13	-1.17 ± 0.18
N3C	8.93 ± 0.02	4.35 ± 0.18	-7.32 ± 0.17
N3D	9.00 ± 0.05	4.04 ± 0.10	-7.81 ± 0.11

[a] Midpoints of the titration curves of ^{15}N chemical shifts vs pH. [b] Errors calculated by curve fitting procedure. [c] Errors are $^1/_2$ peak widths at base.

lations) operating on a Silicon Graphics Indigo-2 workstation.

Distance Calculations. The volume of TRNOE cross-peaks (60 and 90 ms mixing times for butirosin A and isepamicin, respectively) were measured. The observed intensities were classified into three groups based on comparison to the intensity of the TRNOE cross-peak between two protons of known distance ($H1_A$ and $H2_A$, 2.38 Å). Strong, medium, and weak TRNOEs were assigned distance limits of 2.0−2.7 Å, 2.0−3.6 Å, and 2.0−4.5 Å, respectively.

Molecular Dynamics and Minimization. The aminoglycosides were constructed with Insight II (1995 version) (BIOSYM/Molecular Simulations) operating on a Silicon Graphics Indigo-2 workstation. All calculations were carried out using the AMBER force field (*18*) interfaced with the molecular mechanics package DISCOVER (BIOSYM/Molecular Simulations) on the same workstation. The atom potential types and charges of isepamicin and butirosin A were set according to Homans's potential types for carbohydrates (*19*) in the AMBER force field. On the basis of the determined amino group pK_a values for isepamicin (Table 2) and the reported nitrogen pK_a values for butirosin A (*20*), these groups were protonated and given a formal charge of +1.00.

Solution Structure Determination. Random structures of the aminoglycosides were generated by subjecting them to unrestrained dynamics at 600 K for 10.0 ps, with sample structures taken every 1.0 ps. The NOE derived distance restraints were imposed upon the random structures which were then taken through restrained simulated annealing in vacuo. Restrained simulated annealing consisted of a series of restrained conjugate gradient minimizations (500 iterations) followed by restrained molecular dynamics (1.0 ps) at 400, 350, and finally 300 K, with a final restrained conjugate gradient minimization until the rmsd was less than 0.001 kcal/Å. The resulting structures were subjected to restrained molecular dynamics (1.0 ps) at 300 K with water and restrained conjugate gradient minimization with water (500 iterations). These structures were then taken through unrestrained dynamics (1.0 ps) at 100 K with water and a final unrestrained conjugate gradient minimization with water until the rmsd was less than 0.001 kcal/Å. Inclusion of water was performed by enclosing the solute molecule in a box 20 Å × 20 Å × 20 Å and then soaking the volume of the box with solvent water molecules. Periodic boundary conditions were imposed with a nonbonded cutoff distance of 10.0 Å. All molecular modeling calculations of solution structures were carried out with a dielectric constant of 80.0. All force constants for the distance restraints were 50 kcal/mol Å^{-2}.

Enzyme-Bound Structure Determination. Random structures of the aminoglycosides were generated by subjecting them to unrestrained dynamics at 600 K for 10.0 ps, with sample structures taken every 1.0 ps. The TRNOE derived distance restraints were imposed upon the random structures which were then taken through restrained simulated annealing (as described above) followed by unrestrained dynamics at 100 K (1.0 ps) and a final unrestrained conjugate gradient minimization until the rmsd was less than 0.001 kcal/Å. Molecular modeling calculations of enzyme bound structures were carried out in vacuo with a dielectric constants of 4.0 and 80.0 which yielded similar results. All force constants for the distance restraints were 50 kcal/mol Å^{-2}. The dihedral angles for specified groups of structures were averaged to obtain reported values and the standard deviation for the set of dihedral angles was reported.

RESULTS

Kinetic Parameters. Isepamicin is a substrate for AAC-(6′)-Ii with $K_m = 27.8 \pm 4.6$ mM, $k_{cat} = 0.31$ s^{-1}, and $k_{cat}/K_m = 1.1 \times 10^4$ M^{-1} s^{-1}. Substrate inhibition was not observed. The MIC for isepamicin in *E. faecium* C238 was found to be 44 mg/mL, similar to that of kanamycin (*6*). The kinetic parameters of butirosin A for this enzyme were reported to be $K_m = 14.0 \pm 2.6$ mM, $k_{cat} = 0.47$ s^{-1}, and $k_{cat}/K_m = 3.3 \times 10^4$ M^{-1} s^{-1} (*6*). The aminoglycosides shown to be substrates for this enzyme have k_{cat}/K_m values ranging from 0.81×10^4 to 7.2×10^4 M^{-1} s^{-1} (*6*). These low k_{cat}/K_m values have be attributed to the possibility that this enzyme has evolved for the optimal acetylation of other substrates (*6*), although it confers resistance to many aminoglycosides.

Solution Structure of Isepamicin. A total of 30 NOEs were observed for isepamicin in solution, 23 of which were intra-ring and served to define the conformations of individual rings. Four of the observed NOEs were inter-ring and served to define the orientation of the rings with respect to each other. The observed inter-ring NOEs were $H1_A$-$H3_B$, $H1_A$-

Table 3: Statistics of NMR Data and Structures

	AAC(6′)-1i bound butirosin A	AAC(6′)-Ii bound isepamicin	free isepamicin
distance constraints			
total constraints	19	20	30
interring	3	3	4
very strong (1.8 Å)	2	3	4
strong (2.0−2.7 Å)	6	4	7
medium (2.0−3.6 Å)	7	6	12
weak (2.0−4.5 Å)	4	7	7
pairwise rmsd among final structures (Å)			
rings A, B, and C heavy			
all structures	0.18 ± 0.17	0.65 ± 0.59	0.18 ± 0.05
conformer 1		1.33 ± 0.33	
conformer 2		0.44 ± 0.57	
rings A and B heavy			
all structures	0.03 ± 0.01	0.26 ± 0.30	0.12 ± 0.04
conformer 1		0.06 ± 0.02	
conformer 2		0.05 ± 0.04	
pairwise rmsd among random structures (Å)			
rings A, B, and C heavy	1.08 ± 0.20	1.36 ± 0.38	
rings A and B heavy	0.58 ± 0.12	0.50 ± 0.11	

$H4_B$, $H1_C$-$H5_B$, and $H1_C$-$H6_B$. The remaining three NOEs were observed between protons in the D chain. No inter-ring NOEs were observed between rings A and C. From a starting set of 10 random structures, distance restraints derived from NOEs were used in restrained simulated annealing, followed by unrestrained dynamics and energy minimization to arrive at a final set structures. In the set of final structures, all 10 closely resembled each other. Statistics of NMR data and modeled structures are given in Table 3. The glycosidic dihedral angles of isepamicin can be described as ϕ_{AB} ($H1_A$-$C1_A$-O_a-$C4_B$), ψ_{AB} ($H4_B$-$C4_B$-O_a-$C1_A$), ϕ_{BC} ($H1_C$-$C1_C$-O_a-$C6_B$), and ψ_{BC} ($H6_B$-$C6_B$-O_a-$C1_C$). The set of final structures were characterized by $\phi_{AB} = -67.1 \pm 3.5°$, $\psi_{AB} = -58.0 \pm 3.5°$, $\phi_{BC} = -41.6 \pm 2.0°$ and $\psi_{BC} = 60.0 \pm 3.6°$. However, unrestrained molecular dynamics (100 ps at 300 K with inclusion of water) revealed that the solution structure can adopt a range of ϕ_{AB} values from 18.4 to −95.8° with an apparent preferred value of $\phi_{AB} = -29.7 \pm 21.9°$.

AAC(6′)-Ii-Bound Structure of Isepamicin. There were a total of 20 TRNOEs observed for isepamicin in several AAC(6′)-Ii·CoA·isepamicin ternary complexes which contained different ratios of substrate-to-enzyme. Of the observed TRNOEs, 15 were intra-ring and served to define the conformations of individual rings. Three of the observed isepamicin TRNOEs were inter-ring: $H1_A$-$H3_B$, $H1_A$-$H4_B$, and $H1_C$-$H6_B$ (Figure 3). The remaining two TRNOEs were observed between protons in the D chain. No inter-ring NOEs were observed between rings A and C. Simulated annealing, utilizing the TRNOESY derived distance restrains, followed by unrestrained dynamics and energy minimization was used to arrive at final structures from a set of random structures. While the C ring was found to adopt a range of orientations ($\phi_{BC} = -31.2 \pm 33.4°$ and $\psi_{BC} = 31.7 \pm 45.9°$), the structures could be categorized into two groups (conformer 1 and conformer 2) based on the relative positions of the A and B rings with respect to each other. This grouping was based on a qualitative evaluation of ϕ-ψ plots for the A to B glycosidic linkage (data not shown) as well as quantitative evaluation of the rmsd for all the final structures and the groups, respectively (Table 3). It is clear from the data in Table 3 that the A and B ring heavy atom pairwise rmsd values within a conformer group are significantly lower than the value determined for all structures. The dihedral angles that describe the glycosidic linkage between the A and B rings for the two conformers were $\phi_{AB} = -7.9 \pm 2.0°$ and $\psi_{AB} = -46.2 \pm 0.6°$ for conformer 1 and $\phi_{AB} = -69.4 \pm 2.0°$ and $\psi_{AB} = -57.7 \pm 0.5°$ for conformer 2. The grouping of these structures can be seen in Figure 4. Unrestrained molecular dynamics simulations (300 K for 100 ps) demonstrate that conformer 1 and conformer 2 are preferred conformers and are capable of interconverting when monitored at the ϕ_{AB} glycosidic angle (Figure 5), and isepamicin does not significantly populate intermediate values of F. The Y glycosidic angle between rings A and B was observed to stay within a single narrow range during this dynamics calculation (data not shown). Although rotational flexibility exists about the $C5_A$−$C6_A$ bond, the 6_A-amine group of isepamicin seems to occupy significantly different positions in conformer 1 and conformer 2.

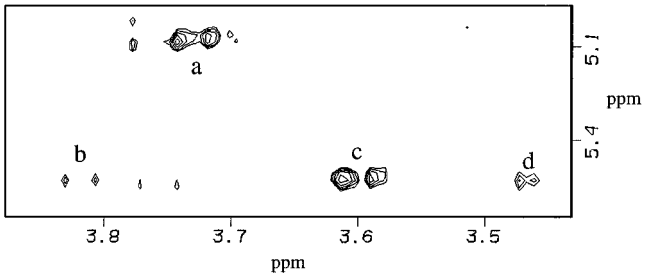

FIGURE 3: A region of the 90 ms TRNOESY spectrum of the AAC(6′)-Ii·CoA·isepamicin ternary complex where AAC(6′)-Ii was 0.30 mM, CoA was 6.0 mM, and isepamicin was 6.0 mM at pH 6.8 in 2 mM Tris-d_{11}. The NOEs indicated are as follows: a, $H1_C$-$H6_B$; b, $H1_A$-$H4_B$; c, $H1_A$-$H2_A$; d, $H1_A$-$H3_B$.

AAC(6′)-Ii-Bound Structure of Butirosin A. We observed 19 TRNOEs for butirosin protons in several AAC(6′)-Ii·CoA·butirosin ternary complexes that contained different ratios of substrate to enzyme, 13 were intra-ring and three were between protons in the D chain. Three of the observed butirosin TRNOEs were inter-ring $H1_A$-$H4_B$, $H1_C$-$H5_B$, and $H2_C$-$H5_B$. No inter-ring NOEs were observed between rings A and C. Simulated annealing, using these restraints, followed by unrestrained dynamics and energy minimization yielded at a set of conformationally similar final structures (Figure 6). The glycosidic dihedral angles of butirosin A can be described as ϕ_{AB} ($H1_A$-$C1_A$-O_a-$C4_B$), ψ_{AB} ($H4_B$-$C4_B$-O_a-$C1_A$), ϕ_{BC} ($H1_C$-$C1_C$-O_b-$C5_B$), and ψ_{BC} ($H5_B$-$C5_B$-O_b-$C1_C$). The modeled structures were characterized by $\phi_{AB} = 0.0 \pm 0.4°$, $\psi_{AB} = 47.1 \pm 0.4°$, $\phi_{BC} = -10.7 \pm 1.7°$, and $\psi_{BC} = -42.3 \pm 0.4°$. CoA did not yield long-range NOEs, and there were no intermolecular NOEs between CoA and butirosin A or isepamicin. Therefore, no structural analysis of CoA was performed.

DISCUSSION

Amine Group pK_a of Isepamicin. Earlier studies have shown that some amine groups of aminoglycosides may have unusually low pK_a values. Therefore, the pK_a values for the amine groups of isepamicin have been determined. Amine groups at the 3_B position of butirosin A (*20*) and isepamicin

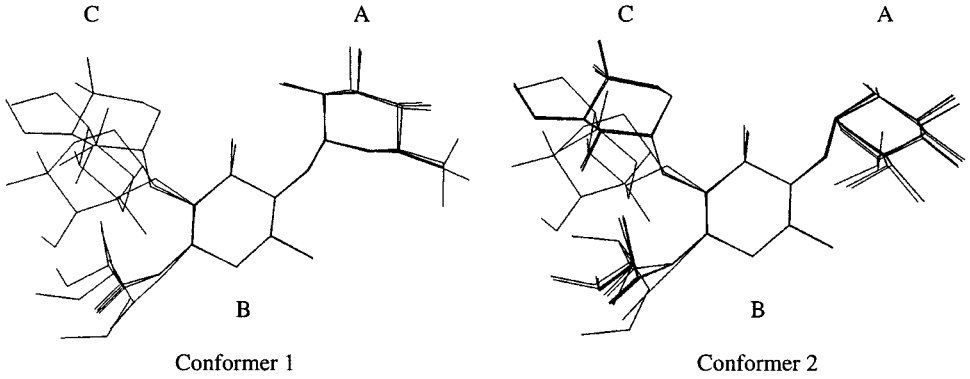

FIGURE 4: Two sets of calculated AAC(6′)-Ii-bound isepamicin structures. The groups are designated conformer 1 (three structures) and conformer 2 (seven structures) as indicated, rings A, B, and C are labeled. These structures were superimposed about the 2-deoxystreptamine ring and the hydrogens have been omitted for simplicity.

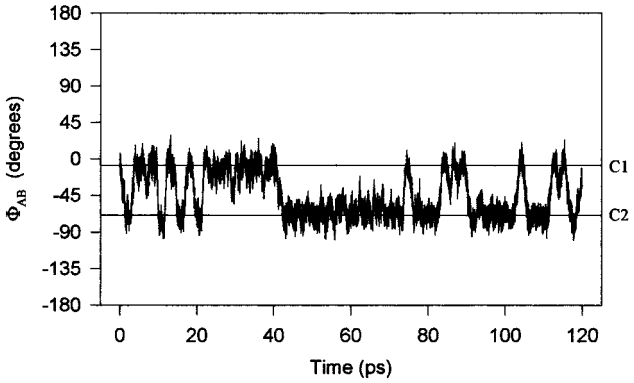

FIGURE 5: The trajectory of the ϕ glycosidic angle between rings A and B of AAC(6′)-Ii-bound isepamicin during the course of a 100 ps unrestrained molecular dynamics at 300 K. The ϕ values for conformer 1 and conformer 2 are indicated as lines labeled C1 and C2, respectively.

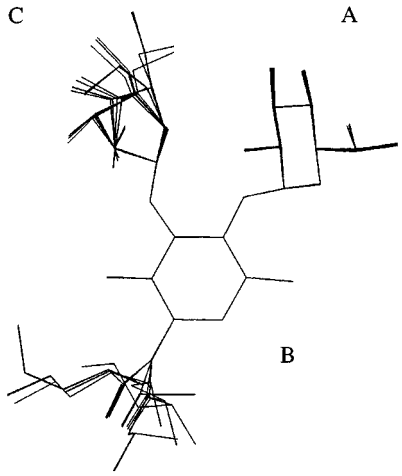

FIGURE 6: The set of 10 calculated AAC(6′)-Ii-bound butirosin A structures. These structures were superimposed about the 2-deoxystreptamine ring and the hydrogens have been omitted for simplicity, rings A, B, and C are labeled.

(this work) have lower pK_as (~7.5) than the expected 8.5−10 range, but not to the extent that was seen with tobramycin (*21*) and neomycin B (*22*). The amine groups of butirosin A and isepamicin were therefore assigned charges of +1.00 based on their pK_as and our experimental conditions for modeling studies. It has been suggested that aminoglycoside−enzyme interactions may be largely electrostatic in nature (*23*, *24*). In this case, those charges may be neutralized upon binding to the enzyme. To assess whether charge interactions were a driving force in our modeling studies of enzyme-bound aminoglycosides, we performed these calculations with dielectric constants of 4.0 (data not shown) and 80.0. The resulting structures were virtually identical. Thus, these calculations were not dominated by Coulombic interactions.

Modeling Strategy. A situation commonly encountered in the conformational analysis of carbohydrate and carbohydrate-like molecules by NMR is a low number of measurable NOEs across glycosidic linkages (*25*). The observed NOEs reflect average values for interactions between nuclei and therefore may not accurately represent torsional variability across the glycosidic linkage. NOE-derived restraints can be used as a guide in molecular modeling calculations to bring the structure to an area of conformational space that agrees with the data. However, the inclusion of restraints in all modeling calculations may cause the structure to be restricted from a local energy minimum forming what can be referred to as a "virtual structure" (*25*). This can be avoided by omitting the restraints in the latter stages of the modeling calculations. Although two different conformations of isepamicin were obtained in simulated annealing, unrestrained dynamics were performed to confirm that these two conformers represent truly distinct structures (Figure 5).

AAC(6′)-Ii-Bound Isepamicin. TRNOE derived distance restraints were used to model the conformation of isepamicin when bound to AAC(6′)-Ii, and two major conformers were observed in the set of final structures (Figure 4). A wide range of orientations were observed for the C ring with respect to the B ring, suggesting that ring C could be flexible when isepamicin is bound to the enzyme. This suggestion is supported by the observation that neamine, which lacks ring C, is a good substrate for this enzyme (*6*). Therefore, ring C of isepamicin may not to be necessary for productive enzyme−substrate complex formation. However, when the orientations of ring A with respect to ring B are examined, two groups of distinct structures emerge. The grouping of these structures were based on the set of F and Y angles observed as well as evaluation of various pairwise rmsd values calculated for the set as a whole and the individual groups (Table 3). Of the 10 modeled structures, three adopted a conformation referred to as conformer 1 and seven adopted a conformation referred to as conformer 2. During unrestrained molecular dynamics simulations (300 K for 100 ps), starting from either a representative of AAC(6′)-Ii-bound isepamicin conformer 1 (Figure 5) or conformer 2 (data not

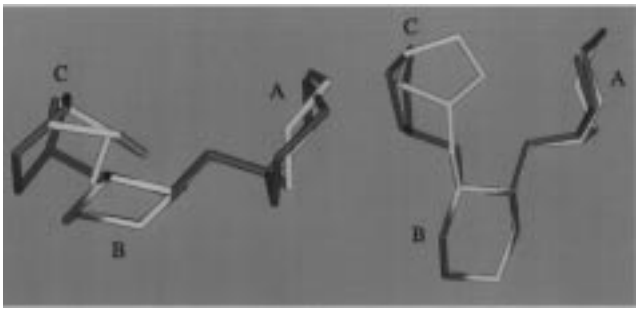

FIGURE 7: Representative AAC(6′)-Ii-bound butirosin A (yellow) and APH(3′)-IIIa-bound butirosin A (red; *20*) ring structures, superimposed at the 2-deoxystreptamine ring, from two different perspectives. For simplicity, the rings have been stripped of their substituents and labeled A, B, and C as indicated.

shown), the two conformers were observed to interconvert by monitoring the ϕ_{AB} glycosidic angle. These studies also showed that conformer 1 and conformer 2 represent preferred conformations, and isepamicin does not adopt intermediate values of ϕ_{AB}. The ψ glycosidic angle between rings A and B was observed to stay within a single narrow range during this dynamics calculation (data not shown). The above results suggest that two conformations of isepamicin may be populated at the active site, and both may be reactive and reflect different binding arrangements. Alternatively, the 6_A amine of isepamicin may be in a reactive position in only one of the conformers and the other represents an unproductive binding mode. A similar situation has been observed for amikacin when bound to APH(3′)-IIIa (*20*) where two sets of enzyme-bound structures were observed. One of the binding modes of AAC(6′)-Ii-bound isepamicin and APH(3′)-IIIa-bound amikacin may represent the antibiotics in unproductive enzyme−substrate complexes. Isepamicin and amikacin remain as two of the more effective aminoglycosides due largely to inefficient inactivation by aminoglycoside modifying enzymes (*26*, *27*). The efficacy of these two antibiotics may, in part, be due to the formation of unproductive enzyme−substrate complexes. However, for AAC(6′)-Ii, there is no kinetic evidence for two binding modes.

AAC(6′)-Ii-Bound Butirosin A. When TRNOE-derived distance restraints were used to model the AAC(6′)-Ii-bound conformation of butirosin A, a set of closely related structures were observed for this antibiotic (Figure 6). Unrestrained molecular dynamics calculations (100 ps at 300 K) revealed that the values of all glycosidic angles fluctuated over single narrow ranges (data not shown). The orientations of the A and C rings, with respect to each other, were found to be orthogonal (Figure 7). A parallel orientation of the A and C rings of butirosin A has been observed in solution structures based on the presence of NOEs between protons of these two rings (*17*). The parallel orientation of rings A and C were also observed for an aminoglycoside phosphotransferase-bound structure of butirosin A (Figure 7; ref *20*). It is known that APH(3′)-IIIa phosphorylates 3_A and 3_C hydoxyl groups of 4,5-disubstituted aminoglycosides such as butirosin A. Thus, both rings need to be properly aligned for phosphorylation in the active site of APH(3′)-IIIa. This may not be necessary for AAC(6′)-Ii-bound butirosin A, since 6_A is the only reactive group. This may explain the difference between the APH(3′)-IIIa-bound and the AAC(6′)-Ii-bound conformations of butirosin A.

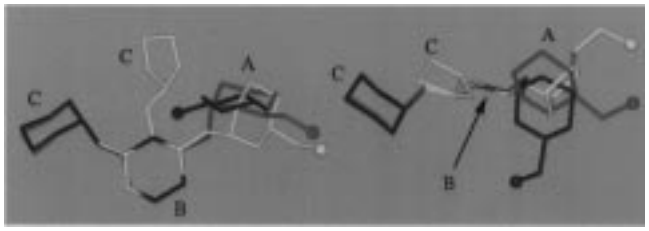

FIGURE 8: Representative structures of AAC(6′)-Ii-bound isepamicin conformer 1 (cyan) and conformer 2 (blue) and AAC(6′)-Ii-bound butirosin A (yellow) from two different perspectives. These structures were superimposed about the 2-deoxystreptamine ring. For simplicity, the rings (labeled A, B, and C as indicated) and have been stripped of their substituents except for the reactive nitrogen at position 6_A which is indicated with a ball in each structure.

Comparison between the set of modeled AAC(6′)-Ii-bound butirosin A structures and the set of enzyme bound isepamicin structures revealed an interesting relationship, the reactive amine can adopt similar positions in isepamicin conformer 1 and butirosin A. Figure 8 shows both conformers of enzyme-bound isepamicin and enzyme-bound butirosin A superimposed about the 2-deoxystreptamine ring. The 2-deoxystreptamine ring is superimposed because it is common to all aminoglycosides and there is a protonated amine group at position 3 which is common to both isepamicin and butirosin A. It has been suggested that protonated amine groups of aminoglycosides participate in ion-pairing interactions that stabilize the enzyme substrate complex for some aminoglycoside modifying enzymes (*23*, *24*). When one considers the rotational freedom about the $C5_A-C6_A$ bond for both aminoglycosides, it is observed that the reactive amine can adopt similar positions in isepamicin conformer 1 and butirosin A. However, the orientations of the A rings are different for conformer 1 of isepamicin and butirosin A. This supports the suggestion by Wright and Ladak (*6*) that 4,5- and 4,6-disubstituted aminoglycosides may bind to AAC(6′)-Ii in different fashions, but the reactive amine is observed to adopt similar spatial orientations in isepamicin and butirosin A when bound to the enzyme. The observed orientation of the 6_A amine group of AAC(6′)-Ii-bound isepamicin conformer 1, when compared to that of enzyme bound butirosin A, lends support to the notion that one of the modeled enzyme bound conformers of isepamicin may represent an unproductive enzyme−substrate complex. Moreover, isepamicin shows a 3-fold lower k_{cat}/K_m value than butirosin A which is consistent with an unproductive bound conformer of isepamicin. On the basis of the relative positioning of the reactive amine group, it is reasonable to suggest that AAC(6′)-Ii-bound isepamicin conformer 1 may represent the productive enzyme−substrate complex.

In conclusion, our results suggest that in the AAC(6′)-Ii·CoA·isepamicin ternary complex, isepamicin adopts two different conformations. On the other hand, butirosin A adopts a single conformation in the AAC(6′)-Ii·CoA·butirosin A ternary complex. Additionally, our observations show that aminoglycosides with 4,6- and 4,5-disubstituted 2-deoxystreptamine rings bind to AAC(6′)-Ii with different conformations. This is similar to what was observed with APH(3′)-IIIa (an aminoglycoside phosphotransferase), and amikacin and butirosin A adopt different conformations in the active site of this enzyme (*28*, *20*). Thus, the active sites of aminoglycoside modifying enzymes may have evolved

to accommodate conformationally different substrates and still achieve regiospecific modification of these substrates.

ACKNOWLEDGMENT

Part of publication costs of this manuscript was covered by an award through the Exhibit, Performance and Publication Expense fund of the University of Tennessee (Knoxville) Office of Research. Special thanks to Dr. J. R. Cox of the University of Tennessee, Knoxville for helpful discussions related to the research presented in this manuscript.

REFERENCES

1. Davies, B. D. (1987) *Microbiol. Rev. 51*, 341−350.
2. Davies, J. (1994) *Science 264*, 375−381.
3. Shaw, K. J., Rather, P. N., Hare, R. S., and Miller, G. H. (1993) *Microbiol. Rev. 57*, 138−163.
4. Umezawa, H., and Kondo, S. (1982) in *Aminoglycoside Antibiotics* (Umezawa, H., and Hooper, I. R., Eds.) pp 267−292, Springer-Verlag, Berlin.
5. Davies, J., and Wright, G. D. (1997) *Trends Microbiol. 5*, 234−240.
6. Wright, G. D., and Ladak, P. (1997) *Antimicrob. Agents Chemother. 41*, 956−960.
7. Davis, D. G., and Bax, A. (1985) *J. Am. Chem. Soc. 107*, 2820−2821.
8. Braunschweiler, L., and Ernst, R. R. (1983) *J. Magn. Reson. 53*, 521−528.
9. Bax, A., and Davis, D. G. (1985) *J. Magn. Reson. 65*, 355−360.
10. Marion, D., and Wüthrich, K. (1983) *Biochem. Biophys. Res. Commun. 113*, 967−974.
11. Bax, A. (1983) *J. Magn. Reson. 53*, 517−520.
12. Rutar, V. (1984) *J. Magn. Reson. 58*, 306−310.
13. Wilde, J. A., and Bolton, P. H. (1984) *J. Magn. Reson. 59*, 343−346.
14. Shaka, A. J., Keeler, J., and Freeman, R. (1983) *J. Magn. Reson. 53*, 313−340.
15. Schanck, A., Brasseur, R., Mingeot-Lecerq, M.-P., and Tulkens, P. M. (1992) *Magn. Reson. Chem. 30*, 11−15.
16. Markley, J. L. (1975) *Acc. Chem. Res. 8*, 70−80.
17. Cox, J. R., and Serpersu, E. H. (1995) *Carbohydr. Res. 271*, 55−63.
18. Weiner, S. J., Kollman, P. A., Nguyen, D. T., and Case, D. A. (1986) *J. Comput. Chem. 7*, 230−252.
19. Homans, S. W. (1990) *Biochemistry 29*, 9110−9118.
20. Cox, J. R., and Serpersu, E. H. (1997) *Biochemistry 36*, 2353−2359.
21. Dorman, D., Paschal, J., and Merkel, K. (1976) *J. Am. Chem. Soc. 98*, 6885−6888.
22. Botto, R. E., and Coxon, B. (1983) *J. Am. Chem. Soc. 105*, 1021−1028.
23. Roestamadji, J., Grapsas, I., and Mobashery, S. (1995) *J. Am. Chem. Soc. 117*, 11060−11069.
24. McKay, G. A., Roestamadji, J., Mobashery, S., and Wright, G. D. (1996) *Antimicrob. Agents Chemother. 40*, 2648−2650.
25. Homans, S. W., and Forster, M. (1992) *Glycobiology 2*, 143−151.
26. Miller, G. H., Sabatelli, F. J., Naples, L., Hare, R. S., and Shaw, K. J. (1995) *J. Chemother. 7* (suppl. 2), 17−30.
27. Miller, G. H., Sabatelli, F. J., Naples, L., Hare, R. S., and Shaw, K. J. (1995) *J. Chemother. 7* (suppl. 2), 31−44.
28. Cox, J. R., McKay, G. A., Wright, G. D., and Serpersu, E. H. (1996) *J. Am. Chem. Soc. 118*, 1295−1301.

BI972778B